

# Combined study of $\text{KNbO}_3$ and $\text{KTaO}_3$ by different techniques of photoelectron and X-ray emission spectroscopy

A. V. Postnikov, B. Schneider, M. Neumann, D. Hartmann, H. Hesse

*Universität Osnabrück – Fachbereich Physik,  
D-49069 Osnabrück, Germany*

A. Moewes

*Center for Advanced Microstructures and Devices at Louisiana State University,  
Baton Rouge, LA 70803, USA*

E. Z. Kurmaev

*Institute of Metal Physics, GSP-170 Yekaterinburg, Russia*

M. Matteucci

*National Research Council, c/o Sincrotrone Trieste, Padriciano 99, I-34012  
Trieste, Italy*

---

## Abstract

The new results are presented of the experimental study of  $\text{KNbO}_3$  and  $\text{KTaO}_3$  by means of X-ray photoelectron spectroscopy, soft X-ray emission and X-ray fluorescence spectroscopy. In particular, Nb  $M_{4,5}$  spectra ( $5p4f \rightarrow 3d_{5/2,3/2}$  transition) have been measured over a range of near-threshold excitation energies 206.5 – 240.6 eV, and Ta  $N_3$  spectra ( $5d6s \rightarrow 4p_{3/2}$  transition) over 399.4 – 420.4 eV at the Beamline 8.0 of the Lawrence Berkeley National Laboratory's Advance Light Source. These spectra were found to be strongly dependent on the excitation energy. Moreover, the O  $K_\alpha$  X-ray emission spectra in both compounds as well as the valence-band photoelectron spectra are brought to the binding energy scale and discussed in combination. The trends in the spectra are explained on the basis of first-principles band-structure calculations, with the dipole transition matrix elements taken into account.

*Key words:* Soft X-ray emission; X-ray photoelectron spectroscopy; electronic structure

---

## Introduction

Potassium niobate and tantalate are traditional benchmark systems for the testing of new theory developments in the study of ferroelectric materials. The starting point of any first-principles treatment, aimed at lattice dynamics or dielectric response, is the knowledge of the ground-state electronic structure. That of  $\text{KNbO}_3$  and  $\text{KTaO}_3$  is believed to be quite well known as a result of a long development beginning with the empirical parameter-adjusting schemes by the end of 1970s [1], followed by first-principles self-consistent treatment [2,3] and finally refined in precision all-electron total energy calculations by different methods [4–6]. In the evaluation of one-electron Kohn-Sham energies, an excellent agreement exists nowadays between different technical implementations of the density functional theory (DFT) – see, for example, Ref. [5–7]. However, the Hartree-Fock formalism provides basically different description of the one-particle excitation spectrum and hence somehow different dielectric constant than that in the DFT treatment [8]. In the situation when *ab initio* calculations of quasiparticle excitations spectra for such moderately complex systems as cubic perovskites are not yet routinely feasible, the electronic and X-ray spectroscopy remains the important tool for the experimental evaluation of the electronic structure data. The X-ray photoelectron spectroscopy (XPS) has been applied in several cases to probe the density of states (DOS) distribution in the valence band (VB) of  $\text{KNbO}_3$  and  $\text{KTaO}_3$  [3,9,10]. Moreover, the angle-resolved ultraviolet photoelectron spectra have been measured for  $\text{KTaO}_3$  and explained in terms of full-potential relativistic theory of photoemission [11]. While being often quite successful in the study of metals, the electron spectroscopy techniques face severe problems in dielectrics due to sample-charging effects. This problem does not arise in the X-ray emission spectroscopy (XES). Larger exit depth of soft X-ray emission, as compared to that of photoelectrons, may be advantageous in many cases because the quality of the sample surface preparation is not so crucial. Moreover, due to dipole selection rules the XES is element-sensitive, which allows to probe partial states distribution related to different atoms. It has been shown that not only DOS but also momentum-resolved information regarding the VB dispersion can be extracted from soft X-ray resonant inelastic spectra (XRIS) [12]. Therefore, XES complements the electron spectroscopy in the study of electronic structure of insulating materials. In the present work, we concentrate on the partial DOS demonstrated by several X-ray emission spectra in  $\text{KNbO}_3$  and  $\text{KTaO}_3$  and analyzed in comparison with the VB XPS. The interpretation of spectra (including the dipole transition matrix elements) was done on the basis of calculations by the all-electron full-potential linearized augmented plane-wave method (FLAPW).

## Experiment and calculation details

The soft X-ray fluorescence experiments were performed at Beamline 8.0 of the Advanced Light Source at Lawrence Berkeley Laboratory. The undulator beamline is equipped with a spherical grating monochromator [13] and the resolving power was set to  $E/\Delta E=500$ . The fluorescence end station with a Rowland circle grating spectrometer provided a resolving power of about 300 at 200 eV. The XPS measurements have been done using a Perkin Elmer PHI 5600ci Multitechnique System with monochromatized Al  $K\alpha$  radiation (bandwidth 0.3 eV FWHM). In order to obtain clean surfaces for the XPS measurements, the  $\text{KNbO}_3$  single crystal was cleaved under UHV conditions. The X-ray Nb  $L\beta_{2,15}$  and Nb  $L\gamma_1$  fluorescence spectra were obtained by a Stearat spectrometer [14]. A quartz crystal ( $d=0.334$  nm) curved to  $R=500$  cm was used as dispersive element to analyze the photons. X-ray emission spectra were detected by a flow proportional counter by scanning along the Rowland circle with an energy resolution of  $\pm 0.2$  eV.

The FLAPW calculations have been done with the WIEN97 implementation of the code [15]. With its extended basis of augmented plane waves, the FLAPW method allows a practical description of the electronic states up to relatively high energies in the conduction band, which is important for analyzing the trends in the X-ray absorption and the resonance X-ray emission intensities [16]. The experimental lattice constant  $a=7.553$  a.u. was used, and the atomic sphere radii were set to 1.95 a.u. (K), 1.85 a.u. (Nb) and 1.65 a.u. (O). The lattice was assumed to be an ideal cubic perovskite because the effect of ferroelectric distortion on the DOS is known to be negligible considering the comparison to experimentally broadened spectra. The local density approximation for the exchange-correlation was used, according to the prescription by Perdew and Wang [17]. The states in the VB have been treated semi-relativistically, the core states fully relativistically. The DOS and emission spectra were calculated using the tetrahedron method, for the  $12 \times 12 \times 12$  divisions of the whole Brillouin zone. Whereas our calculated partial and total DOS agree with previous calculations cited above, the calculated X-ray emission (and absorption) spectra, including the energy dependence of the dipole transition matrix elements present, to our knowledge, new information. We utilize our calculated results to understand the trends in our resonant X-ray emission spectra.

## Results and discussion

In Fig. 1 the Nb  $M_{4,5}$  emission spectra of  $\text{KNbO}_3$  are shown for various excitation energies near the Nb3d threshold. Four features are observed and labeled

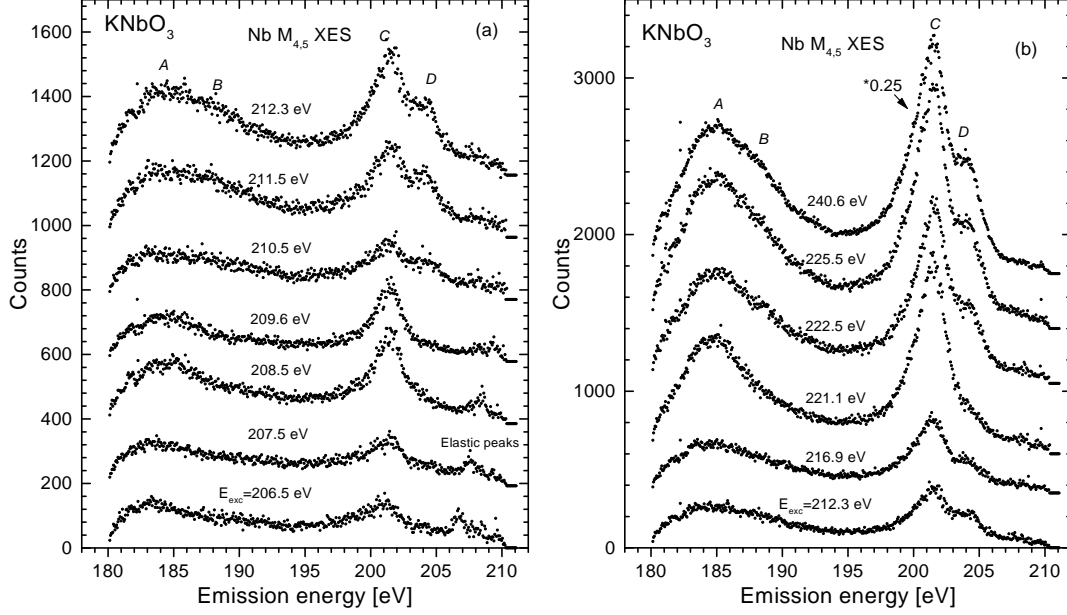


Fig. 1. Nb  $M_{4,5}$  emission spectra of  $\text{KNbO}_3$ . The excitation energy is tuned through the Nb  $3d$ -threshold from 206.5 to 212.3 eV (a) and from 212.3 to 240.6 eV (b).

*A* through *D*. The most dramatic changes in the fine structure of Nb  $M_{4,5}$  emission spectra are found for excitation energies between 206.5 and 212.3 eV where new features *B* and *D* appear with changes in excitation energy. It was suggested in Ref. [18] that the Nb  $M_{4,5}$  emission only reveals the  $M_5$  ( $3d_{5/2}$ ) features because the  $M_4$  ( $3d_{3/2}$ ) is filled by radiationless transition. Therefore it was unexpected when we found the excitation energy dependence of Nb  $M_{4,5}$  to be distorted by the spin-orbit splitting of the Nb  $3d$ -levels and hence the band dispersion effects to be blurred.

Fig. 2 displays the calculated Nb  $M_{4,5}$  emission spectra based on the Nb $5p$  and Nb $4f$  DOS and modulated by the dipole transition probabilities. The resulting spectrum consists of two (identical) contributions, corresponding to individual  $M_4$  and  $M_5$  spectra, that have been shifted apart by the value of the calculated Nb $3d$  spin-orbit splitting (2.88 eV) and summed up with relative weights 2:3. It was found that the contribution of the Nb $4f$  states is negligible in the VB, so that only the  $5p \rightarrow 3d$  transition is important for the interpretation of the Nb  $M_{4,5}$  XES. The  $O2s$  states contribute to the Nb  $M_5$  XES due to the  $O2s$ -Nb $5p$  hybridization. The corresponding features in the Nb  $M_4$  and  $M_5$  XES near  $-16$  eV and  $-13$  eV are broadened in the experimental spectra but still recognizable in Fig. 1 as peaks *A* and *B*.

Going back to the discussion of the energy dependence of the Nb  $M_{4,5}$  emission spectra (Fig. 1), we note that according to our XPS measurements the Nb  $M_5$  ( $3d_{5/2}$ ) and Nb  $M_4$  ( $3d_{3/2}$ ) binding energies are 207.23 and 210 eV, respectively (relative to the vacuum level). Conclusively the emission features in the spectra excited between 206.5 and 209.6 eV are generated by the refill of the Nb

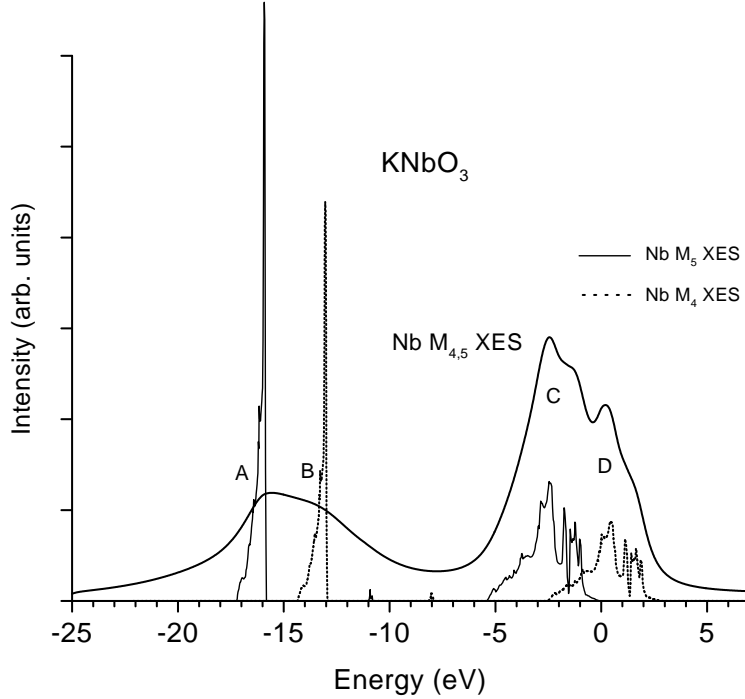


Fig. 2. Calculated Nb  $M_{4,5}$  XES of  $\text{KNbO}_3$  broadened for instrumental broadening (0.2 eV), core level life-time (0.35 eV) and valence life-time (2.0 eV). The contributions of unbroadened  $M_5$  and  $M_4$  spectra are also shown.

$M_5(3d_{5/2})$  hole because the excitation of Nb  $M_4$  is not possible below 210 eV. In the excitation energy range between 210.5 and 216.9 eV, additional features  $B$  and  $D$  appear as a result of contributing transitions to Nb  $M_4(3d_{3/2})$ . The sharp increase in intensity in the emission spectra at excitation energies from 216.9 eV to 221.1 eV can be attributed to the threshold of the  $3d \rightarrow 4f$  absorption. This is illustrated by the calculated Nb  $M_4$  absorption spectrum in Fig. 3. The onset for the  $3d \rightarrow 4f$  absorption occurs around 235 eV. Whereas the  $3d \rightarrow 4f$  contribution dominates in the  $M_{4,5}$  absorption spectrum, the  $3d \rightarrow 5p$  process gives rise to the absorption at about 218 eV. The strong enhancement of the emission (see Fig. 1) occurs when the excitation energy exceeds the  $M_5$  threshold ( $E_{exc}=208.5$  eV),  $M_4$  threshold ( $E_{exc}=211.5$  eV) and the  $3d - 5p$  threshold ( $E_{exc}=221.1$  eV) as displayed in the absorption spectrum (Fig. 3). This sharp increase in the absorption intensity and hence in the resonant emission appears in each of these steps, at increase of the excitation energy, first for the  $M_5$  component and followed by the  $M_4$ . The emission spectrum corresponding to the excitation energy of 221.1 eV in Fig. 1 exhibits, as compared with that for  $E_{exc}=216.9$  eV, strongly enhanced  $M_5$  but relatively unchanged  $M_4$  intensity. Therefore, this specific selective excitation of Nb  $M_5$  XES can be also used to receive experimental information about Nb  $5p$  DOS undistorted by overlapping with the Nb  $M_4$  XES.

Apart from Nb  $M_{4,5}$ , some other XES measurements are useful to provide complementary information about the electronic state distribution at the Nb

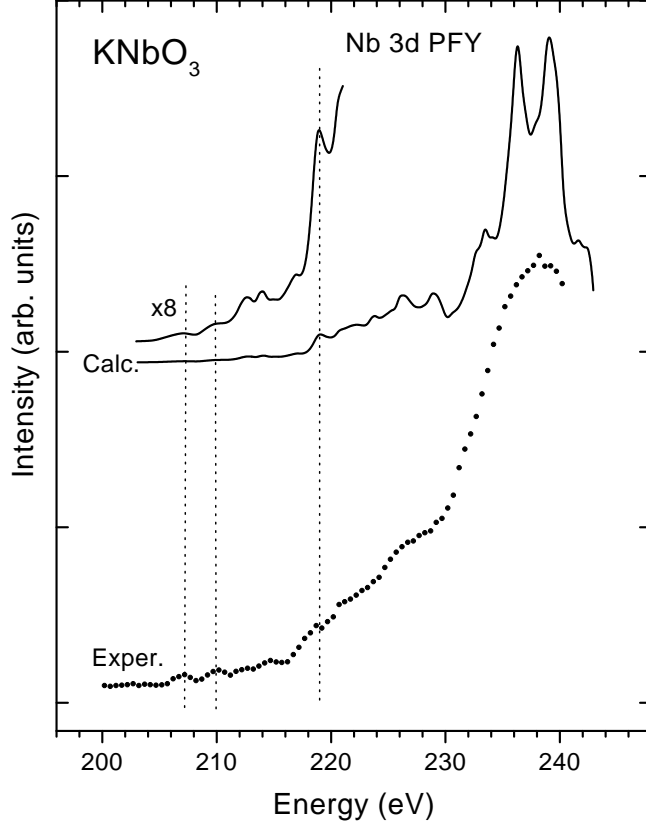


Fig. 3. Calculated and measured Nb  $3d \rightarrow 5p$  partial fluorescence yield (PFY).

site. In Fig. 4, Nb  $M_3$  ( $4d \rightarrow 3p_{3/2}$ ), Nb  $L\beta_{2,15}$  ( $4d_{5/2,3/2} \rightarrow 2p_{3/2}$ ) and Nb  $\gamma_1$  ( $4d_{3/2} \rightarrow 2p_{1/2}$ ) spectra are shown in comparison with the VB XPS. The spectra are brought to a common scale of binding energies, based on the binding energies of corresponding core levels. Since  $M_4$  and  $M_5$  spectra cannot be easily separated, they are plotted with respect to the  $3d_{5/2}$  binding energy (207.23 eV). The Nb  $M_{2,3}$  spectra have not been, to our knowledge, measured before, since they were not listed in the Bearden tables [19], nor in the last systematic study of the ultrasoft XES in  $4d$ -transition metals [20]. These spectra lie in a convenient energy region for the synchrotron study, and their two components ( $3p_{1/2}$  and  $3p_{3/2}$ ) are well separated by  $\approx 15$  eV. The  $M_3$  spectrum shown in Fig. 4 was obtained in an exposition time of about 20 min. Despite their low intensity, the  $M_{2,3}$  spectra may be potentially suitable for the study of the VB, probably including dispersion effects. The overall difference between Nb $M_3$  and Nb $L$  spectra on one hand and the Nb  $M_{4,5}$  spectra on the other hand is that the former probe primarily the occupied Nb $4d$  DOS, centered near the VB bottom, whereas the latter reveal the contribution of the occupied states with the  $l=1$  symmetry at Nb site, that are diffuse and hybridize strongly with VB states of other atoms. It is well seen from Fig. 4 that on the common energy scale, the maximum of the  $M_5$  spectrum lies roughly in the middle of the VB. The energy positioning of the O  $K_\alpha$  spectrum in the common energy scale has been done based on the O1s binding energy (530.1 eV). This spectrum reveals

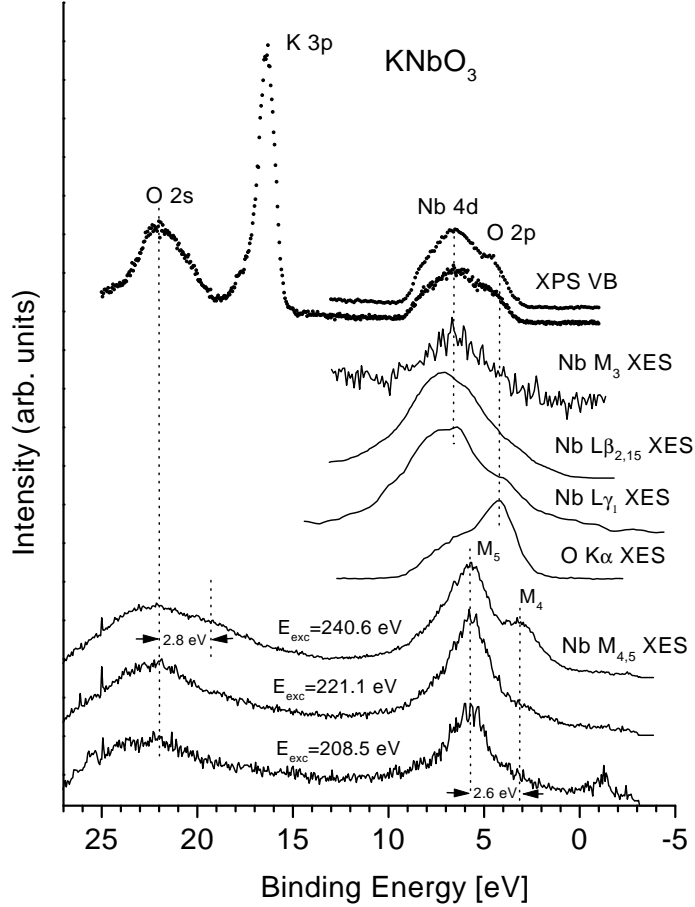


Fig. 4. The comparison of valence band photoemission (XPS VB), O  $K\alpha$ -emission and several Nb XES in  $\text{KNbO}_3$ .

the predominant distribution of  $\text{O}2p$  states near the top of the VB – the fact well known from band structure calculations (see, for example, Ref. [5]). The shape of the spectrum shows no development as the excitation energy varies, the reason being that no vacant  $\text{O}2p$  states are available near the bottom of the conduction band, so that the O  $K\alpha$  emission is essentially incoherent with the corresponding absorption. The  $3p$  state of potassium does not hybridize with any of the states contributing to the spectra above discussed and is visible only in the XPS.

Potassium tantalate has been earlier studied by XPS in comparison with potassium niobate [3,9]. In the present work, we concentrate on the Ta  $N_{2,3}$  ( $5d6s \rightarrow 4p_{3/2,1/2}$ ) emission spectra that have not been reported before. The  $M_2$  and  $M_3$  spectra are far separated in energy (by  $\approx 62$  eV) and probe primarily the Ta states well represented in the VB and at the bottom of the conduction band. As is known from the calculated band structure (see Ref. [5,7]), these bands exhibit strong energy dispersion. In Fig. 5, the sequence of Ta  $N_3$  is shown for several excitation energies, obtained at 5–10 min. exposure per spectrum. The intensity is therefore much higher than that of counterpart  $M_{2,3}$

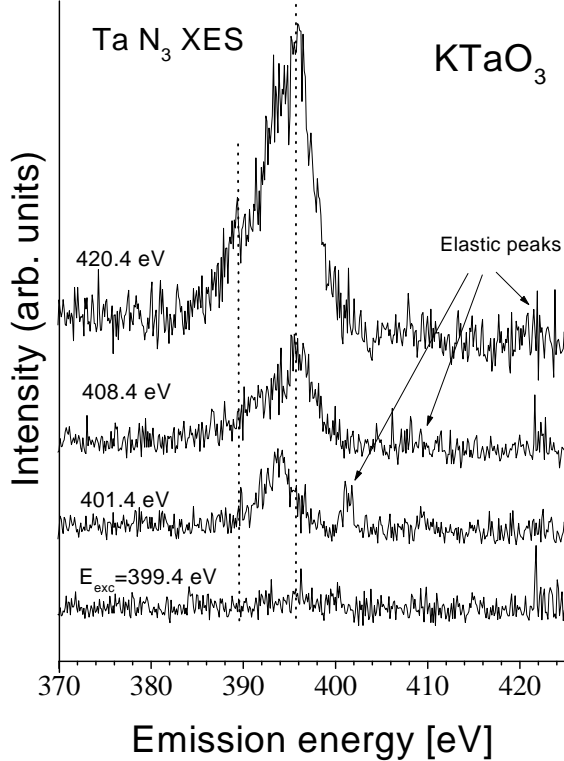


Fig. 5. Ta  $N_3$  X-ray emission spectra of  $\text{KTaO}_3$  for four excitation energies.

spectra in  $\text{KNbO}_3$ . Moreover, some development may be seen in the spectra depending on the excitation energy. While still absent at  $E_{exc}=399.4$  eV, the X-ray emission is clearly visible at  $E_{exc}=401.4$  eV, i.e. well below the  $\text{Ta}4p_{3/2}$  excitation energy (404.0 eV). The displaced peak position at  $E_{exc}=401.4$  eV. may be an indication of the X-ray resonant Raman scattering [22] that enables excitations just below the threshold. Similar trends have been observed in Ref. [23] below and through the Ti  $L_3$  absorption threshold in another perovskite system  $(\text{Ba,Sr})\text{TiO}_3$ .

The XPS of  $\text{KTaO}_3$  does not differ much from earlier studies [3,9]. The O  $K_\alpha$  emission spectrum is similar (but not completely identical) to that in  $\text{KNbO}_3$ . A separate analysis of our spectroscopy studies on  $\text{KTaO}_3$  will be described elsewhere [21].

Summarizing, we have compared the available spectroscopic experimental information about electronic structure of  $\text{KNbO}_3$  (including new Nb  $M_{4,5}$  XES, Nb  $L\beta_{2,15}$ , Nb  $L\gamma_1$ , O  $K_\alpha$  XES and the VB XPS with the results of first-principles calculations. The contributions from decay of the  $3d_{5/2}$  and  $3d_{3/2}$  holes via valence emission are attributed by tuning the excitation energy. In terms of the spectra being potentially suitable for the study of band dispersion in the perovskites in question, we found that Nb  $M_{2,3}$  have very low intensity whereas the two components of Nb  $M_{4,5}$  are strongly overlapped which complicates the analysis. The Ta  $N_{2,3}$  spectra are apparently free from both



these disadvantages. The implications for the structural studies in perovskites may be – provided the band dispersion studies turn out to be successful – the analysis of the band structure distortion in lower-symmetry phases with the use of angle-resolved resonance X-ray emission.

## Acknowledgements

This work was supported by the Russian Science Foundation for Fundamental Research (Project 96-15-96598 and 98-02-04129), the NATO Linkage Grant (HTECH.LG 971222), the DFG-RFFI Project, the Swedish Natural Science Research Council (NFR) and the Göran Gustavsson Foundation for Research in Natural Sciences and Medicine. AVP, BS and MN acknowledge the support of the German Research Society (SFB 225).

## References

- [1] P. Pertosa, F. M. Michel-Calendini, and G. Metrat, *Ferroelectrics* **21**, 637 (1978); P. Pertosa and F. M. Michel-Calendini, *Phys. Rev. B* **17**, 2011 (1978).
- [2] Yong-Nian Xu, W. Y. Ching and R. H. French, *Ferroelectrics* **111**, 23 (1990).
- [3] T. Neumann, G. Borstel, C. Scharfschwerdt, and M. Neumann, *Phys. Rev. B* **46**, 10623 (1992).
- [4] D. J. Singh and L. L. Boyer, *Ferroelectrics* **136**, 95 (1992).
- [5] A. V. Postnikov, T. Neumann, G. Borstel, and M. Methfessel, *Phys. Rev. B* **48**, 5910 (1993).
- [6] R. D. King-Smith and D. Vanderbilt, *Phys. Rev. B* **49**, 5828 (1994).
- [7] D. J. Singh, *Phys. Rev. B* **53**, 176 (1996).
- [8] L. Fu, E. Yaschenko, L. Resca, and R. Resta, *Phys. Rev. B* **57**, 6967 (1998).
- [9] A. Winiarski, T. Neumann, B. Mayer, G. Borstel, and M. Neumann, *phys. stat. sol. (b)* **183**, 475 (1994).
- [10] L. Douillard, F. Jollet, C. Bellin, M. Gautier, and J. P. Duraud, *J. Phys.: Condens. Matter* **6**, 5039 (1994).
- [11] M. Grass, J. Braun, A. Postnikov, G. Borstel, H. Ünlü, and M. Neumann, *Surf. Sci.* **352-354**, 760 (1996).

- [12] Y. Ma, N. Wassdahl, P. Skytt, J. Guo, J. Nordgren, P. D. Johnson, J.-E. Rubensson, T. Boske, W. Eberhardt, and S. D. Kevan, *Phys. Rev. Lett.* **69**, 2598 (1992); J. A. Carlisle, E. L. Shirley, E. A. Hudson, L. J. Terminello, T. A. Callcott, J. J. Jia, D. L. Ederer, R. C. C. Perera, and F. J. Himpsel, *Phys. Rev. Lett.* **74**, 1234 (1995); S. Shin, A. Agui, M. Watanabe, M. Fujisawa, Y. Tezuka, and T. Ishii, *Phys. Rev. B* **53**, 15660 (1996); P. D. Johnson and Y. Ma, *Phys. Rev. B* **49**, 5024 (1994); J. Lüning, J.-E. Rubensson, C. Ellmers, S. Eisebitt, and W. Eberhardt, *Phys. Rev. B* **56**, 12147 (1997).
- [13] J. J. Jia, T. A. Callcott, J. Yurkas, A. W. Ellis, F. J. Himpsel, M. G. Samant, G. Stöhr, D. L. Ederer, J. A. Carlisle, E. A. Hudson, L. J. Terminello, D. K. Shuh, and R. C. C. Perera, *Rev. Sci. Instrum.* **66** (2), 1394 (1995).
- [14] V. E. Dolgih, V. M. Cherkashenko, E. Z. Kurmaev, *Pribory and Technika Experimenta (USSR)* No. 6 (1983), p. 2517.
- [15] P. Blaha, K. Schwarz, and J. Luitz, **WIEN97**, Vienna University of Technology 1997. Improved and updated Unix version of the original copyrighted WIEN-code, which was published by P. Blaha, K. Schwartz, P. Sorantin, and S. B. Trickey, *Comput. Phys. Commun.* **59**, 399 (1990).
- [16] The use of the density functional theory-based schemes for the description of excited electronic states has no justification but is widely used in practice. From the experience based on quasiparticle calculations available for some oxide systems, one can expect an almost uniform energy shift accompanied by some slight distortion of empty energy bands as a result of switching from LDA to a quasiparticle calculation. Moreover, the linearization error of the LAPW method may become noticeable within the energy range of  $\approx 40$  eV used in the present calculation of the absorption spectra. One can expect, however, that the hierarchy of excitation peaks is described qualitatively correctly by the LDA in the vicinity of the absorption threshold.
- [17] J. P. Perdew and Y. Wang, *Phys. Rev. B* **45**, 13244 (1992).
- [18] A. P. Lukirskii and T. M. Zimkina, *Izv. AN SSSR, ser. fiz.* **27**, 330 (1963).
- [19] J. A. Beardeen, *Rev. Mod. Phys.* **39**, 78 (1967).
- [20] V. A. Fomichev, T. M. Zimkina, A. V. Rudnev, and S. A. Nemnonov, *Band Structure Spectroscopy of Metals and Alloys* (ed. By D. J. Fabian and L. M. Waton), Academic Press, London and New York, 1973, p. 259.
- [21] B. Schneider, M. Matteucci, A. V. Postnikov, E. Z. Kurmaev, A. Moewes, V. V. Fedorenko, D. Hartmann, H. Hesse and M. Neumann, to be published.
- [22] T. Åberg and B. Crasemann, *Resonant Anomalous X-ray Scattering* (ed. by G. Materlik, C. J. Sparks and K. Fischer), Elsevier Science, 1994, p.431; T. Minami and K. Nasu, *Phys. Rev. B* **57**, 12084 (1998)
- [23] Y. Uehara, D. W. Lindle, T. A. Callcott, L. T. Terminello, F. J. Himpsel, D. L. Ederer, J. H. Underwood, E. M. Gullikson and R. C. C. Perera, *Appl. Phys. A* **65**, 179 (1997).